GEOPHYSICAL RESEARCH LETTERS, VOL. 40, 5861–5866, doi:10.1002/2013GL058081, 2013

Layered structure of the lithospheric mantle changes dynamics of craton extension

J. Liao,[1] T. Gerya,[1] and Q. Wang[2]

Received 20 September 2013; revised 6 November 2013; accepted 6 November 2013; published 27 November 2013.

[1] Although presence of weak layers due to hydration and/or metasomatism in the lithospheric mantle of cratons has been detected by both geophysical and geochemical studies, its influence on craton evolution remains elusive. Using a 2-D thermomechanical viscoelastoplastic numerical model, we studied the craton extension of a heterogeneous lithospheric mantle with a rheologically weak layer. Our results demonstrate that the effect of the weak mantle layer is twofold: (1) enhances deformation of the overlying lithosphere and (2) inhibits deformation of the underlying lithospheric mantle. Depending on the weak-layer depth, the Moho temperature and extension rate, three extension patterns are found (1) localized mantle necking with exposed weak layer, (2) widespread mantle necking with exposed weak layer, and (3) widespread mantle necking without exposed weak layer. The presence of the weak mantle layer reduces long-term acting boundary forces required to sustain extensional deformation of the lithosphere. **Citation:** Liao, J., T. Gerya, and Q. Wang (2013), Layered structure of the lithospheric mantle changes dynamics of craton extension, *Geophys. Res. Lett.*, *40*, 5861–5866, doi:10.1002/2013GL058081.

1. Introduction

[2] Physical parameters controlling the stability and destruction of cratons remain hotly debated [*Sleep*, 2005; *Lee et al.*, 2011; *Gerya*, 2012, and references therein]. Based on numerical thermomechanical models, positive chemical buoyancy, high viscosity and high yield strength of the cratonic lithosphere are regarded as the key factors that ensure the long-term craton stability under the condition of an ongoing mantle convection [*Lenardic and Moresi*, 1999; *Lenardic et al.*, 2000, 2003; *O'Neill et al.*, 2008; *Peslier et al.*, 2010; *Yoshida*, 2012]. Indeed, previous numerical studies typically assumed a homogeneous lithospheric mantle structure under cratons. This assumption has recently been challenged by a heterogeneous layered structure of the cratonic mantle lithosphere detected from both geophysical and geochemical studies [*Thybo and Perchuc*, 1997; *Griffin et al.*, 2004; *Peltonen and Brügmann*, 2006; *Thybo*, 2006; *Romanowicz*, 2009; *Rychert and Shearer*, 2009; *Fischer et al.*, 2010; *Yuan and Romanowicz*, 2010; *Abt et al.*, 2010]. The strong, scattered reflections beyond 8° offset in all continental high-resolution, long-range seismic profiles identify a low velocity zone (LVZ) at ∼100 km depth in the continental mantle [*Thybo and Perchuc*, 1997; *Thybo*, 2006]. The global presence of this LVZ beneath Precambrian shields and platforms is confirmed by high-frequency P-to-S (Ps) converted phases at depths of 95±4 km [*Rychert and Shearer*, 2009]. Such sharp velocity drop cannot be caused by temperature alone because of the nearly constant occurrence depth in both hot and cold areas, and it is too shallow to be related with the lithosphere-asthenosphere boundary (LAB) as the LAB beneath cratons generally reach 200–250 km [*Romanowicz*, 2009; *Eaton et al.*, 2009]. Geochemical data of mantle xenoliths indicate that the lithospheric mantle beneath Slave Craton consists of a depleted upper layer and a refertilized lower layer, with a boundary at 140–160 km [*Griffin et al.*, 2004]. This two-layer structure is consistent with changes in the direction of azimuthal anisotropy with depth in the North American Craton [*Yuan and Romanowicz*, 2010].

[3] The nature and tectonic implications of this sharp midlithospheric boundary challenge our understanding on the craton evolution. Several effects that may contribute to the generation of this midlithospheric LVZ have been summarized by *Thybo* [2006]. The favorite hypothesis for the LVZ is partial melting of peridotites because even small amount of melt or fluids (< 1 to 2%) can significantly decrease seismic velocities of peridotites [*Thybo and Perchuc*, 1997; *Karato and Jung*, 1998; *Thybo*, 2006]. However, the lack of correspondent high conductivity layer caused by partial melting [*Maumus et al.*, 2005] beneath cratons makes people argue the wide presence of a partially molten layer at depth of 100 km. It is noteworthy that Archean lithospheric mantle have been strongly affected by Proterozoic and Phanerozoic melt-related metasomatism [*Griffin et al.*, 2003, 2004; *Sleep*, 2009]. The continental lithospheric strength can be dramatically reduced if metasomatism and/or subduction-related hydration occur over wide areas in the mantle [*Hacker et al.*, 2003; *Carlson et al.*, 2005; *Wang*, 2010; *Lee et al.*, 2011; *Wang et al.*, 2013], and the depth of the weakened area is related with the peak of the lithospheric strength envelop, because ascending magma dikes cannot penetrate the strongest lithospheric part and freeze at that depth [*Sleep*, 2009].

[4] Although the origin of the LVZ is still not clear, it may correspond to a weak zone in the upper mantle because of hydration, metasomatisim, or partial melt. So far, only a few modeling studies take into account the lithospheric mantle heterogeneity [*O'Neill et al.*, 2010]. In this paper, we investigate cratonic extension processes superimposed on a heterogeneous lithospheric mantle structure containing

Additional supporting information may be found in the online version of this article.

[1]Geophysical Fluid Dynamics, Institute of Geophysics, Zurich, Switzerland.
[2]State Key Laboratory for Mineral Deposits Research, Department of Earth Sciences, Nanjing University, Nanjing, China.

Corresponding author: J. Liao, Geophysical Fluid Dynamics, Institute of Geophysics, ETH Zurich, Sonneggstrasse 5, CH-8092, Zurich, Switzerland. (jie.liao@erdw.ethz.ch)

0094-8276/13/10.1002/2013GL058081

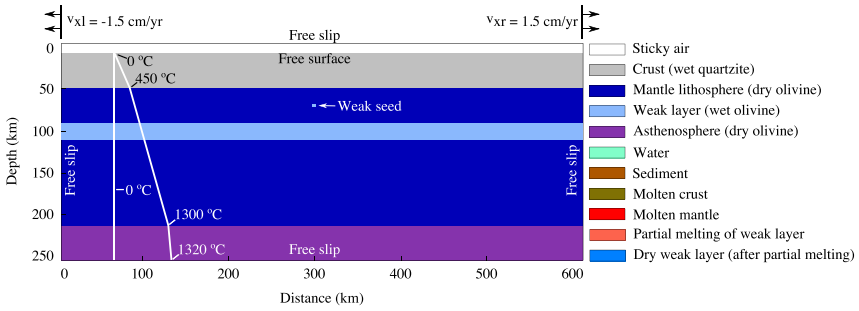

Figure 1. Initial setup for the reference model. A 10 km thick "sticky air" is used to make the crustal surface a free surface [*Crameri et al.*, 2012]. Initial temperature in the model is uniform laterally and increases linearly in the crust and lithospheric mantle with different gradients due to the prescribed Moho temperature (white lines in the figure). Lithosphere-asthenosphere boundary has an initial temperature of 1300°C, below which asthenosphere is adiabatic with an initial temperature gradient 0.5°C/km. Extension rate of 1.5 cm/yr (half rate) is prescribed symmetrically on left and right boundaries. Compensating vertical influx velocities through the upper and lower boundaries is imposed to ensure mass conservation in the model domain and constant average 10 km thickness of the sticky air layer. A weak seed is imposed to localize deformation in the model domain [*Huismans and Beaumont*, 2011].

a rheologically weak layer (hereby "layered model") and compare results to extension of a homogeneous lithospheric mantle (hereby "homogeneous model"). In addition, we test sensitivity of layered model extension to the weak-layer depth, the Moho temperature and extension rate.

2. Numerical Model Description

[5] The numerical model setup is shown in Figure 1, and more detailed description of numerical implementation can be found in the supporting information. Governing momentum, mass, and heat conservation equations are solved with the 2-D thermomechanical viscoelastoplastic numerical code I2ELVIS based on finite-difference method and marker-in-cell techniques [*Gerya and Yuen*, 2007].

3. Modeling Results

3.1. Reference Models

[6] Figure 2 (and Figure S1 in the supporting information) compares extension dynamics for homogeneous and layered models for an extension rate of 1.5 cm/yr (half rate). In the homogeneous model, brittle deformation is dominant in the early stage while ductile deformation becomes dominant after a certain extension. Brittle deformation generates asymmetric shear zones in the upper lithosphere and leads to the formation of asymmetric grabens/half grabens on the surface (Figures 2a–2b). Shear heating causes asymmetric extension, as it produces significant temperature perturbations (Figure 2b). Symmetric mantle necking becomes dominant gradually, and as a result, relatively symmetric topography forms (Figures 2c and 2d). With further extension, decompression melting is generated followed by the lithospheric breakup (t = 10.1 Ma, Figures 2e and 2f). Relatively symmetric passive margins develop on the two sides of the breakup.

[7] Our layered model has an identical setup to the homogeneous model, except for a 20 km thick weak layer at depth of 90 km. The layered model has notably different extension dynamics (Figures 2g–2l) compared to the homogeneous model described above. In the early extension stage (t = 2.1 Ma, Figures 2g and 2h), the weak-layer flows toward the extension center and forms a dome which can rupture the overlying mantle and crust rapidly. Due to the enhanced deformation in the upper lithosphere, the surface is subjected to deep depressions. After a certain period of extension (t = 6.1 Ma, Figures 2i and 2j), the crust has been broken apart by the weak layer, while the lithospheric mantle located underneath the weak layer remains relatively undeformed. Thus, the presence of the weak layer accelerates deformation of the overlying lithosphere, but inhibits deformation of the underlying lithosphere and upwelling of the asthenosphere. A possible explanation is that the flow of the weak layer toward the extension center accommodates the space generated by extension, which prevents the mantle upwelling beneath the weak material (Figures S1f–S1h). Asymmetric mantle necking occurs at the tips of the major shear zones which are formed related to a channel flow of weak material (Figures 2j, S1h, and S1i). As a consequence, the asymmetric distribution of depressions on the surface is enhanced. Finally (t = 10.1 Ma, Figures 3k and 3l), an asymmetric localized mantle necking dominates the lithospheric deformation, generating asymmetric continental breakup and passive margins. The difference of the mean lithospheric strength (Figures 2m–2o, averaging the second invariant deviatoric stress horizontally) between the homogeneous and layered models is mainly caused by the accumulation of the weak layer. We name the deformation pattern of the layered model as localized mantle necking with exposed weak layer. In the next section, we will investigate controlling parameters on the formation of widespread mantle necking with or without exposed weak layer.

3.2. Influence of Model Parameters

[8] Here we test influences of the weak-layer depth, the Moho temperature, and extension rate on cratonic extension patterns. The weak-layer depth controls the transition from localized mantle necking to widespread mantle necking. Wider mantle necking is favored by a deeper weak layer (Figures 3a and S2a–S2f) because the location of major shear zones before mantle necking is controlled by the weak layer. The deeper the weak layer locates, the deeper the major shear zones (detachments) reach. These shear zones localize large strain and widen the mantle upwelling area.

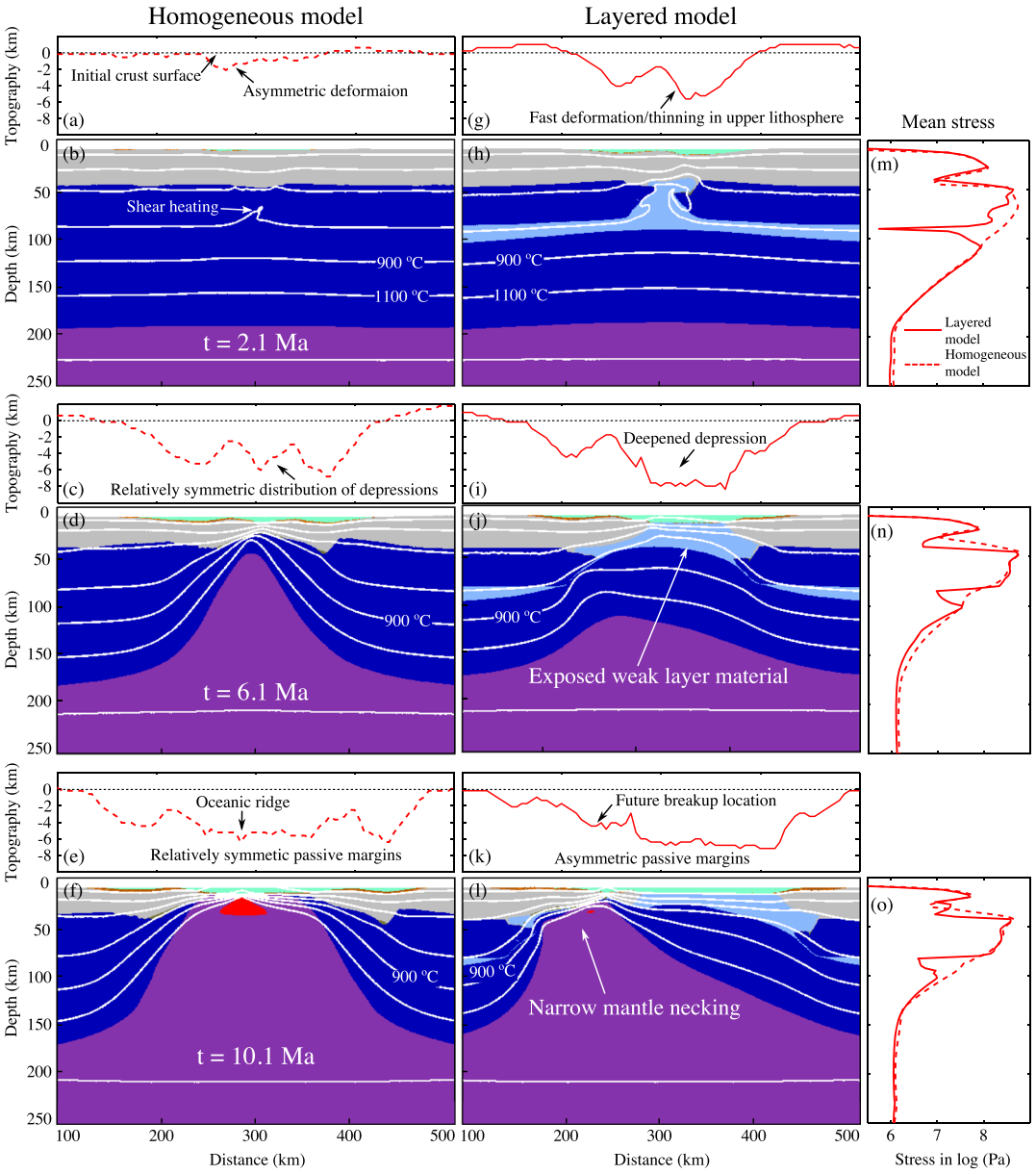

Figure 2. Extension of layered and homogeneous model at times of 2.1, 6.1, and 10.1 Ma. (a, c, e, g, i, k) Topography, (b, d, f, h, j, l) composition, and (m, n, o) second invariant deviatoric stress are compared for both models. White lines in the composition snapshots are isotherms, with an interval of 200°C. Parameters used in the layered model are depth = 120 km (depth of the upper surface of the weak layer), T_{Moho} = 450°C (Moho temperature), velocity = 1.5 cm/yr (half-extension rate). Note the deformation pattern: weak layer is exposed to the surface and localized mantle necking is generated (localized mantle necking with exposed weak layer).

Consequently, the deformation pattern is widespread mantle necking with exposed weak layer. Moho temperature also affects the rifting patterns because it controls the strength ratio between crust and mantle. In agreement with the previous study [*Gueydan et al.*, 2008], a low Moho temperature promotes narrow rifting while a high Moho temperature favors wide rifting. Higher Moho temperatures generate more widespread extension in both homogeneous and layered models, and strain localization occurs later (Figures 3b, S3, and S5). Compared to the homogeneous model, the layered model results in more diffused deformation. High Moho temperatures favor the deformation pattern of widespread mantle necking with exposed weak layer. Moreover, extension velocities prescribed on the side boundaries could play an important role because effective viscosity is strain-rate dependent. With a slow extension rate (0.3 cm/yr, half rate), the weak layer does not erupt to the surface, but distributes along the Moho, which results in widespread mantle necking without exposed weak layer (Figures 3e and S4a–S4f). For faster extension, weak layer always breaks apart the overlying rock and the lithospheric extension is characterized by localized mantle necking with exposed weak layer (Figures S4g–S4l and S5).

3.3. Boundary Force

[9] To examine the evolution of the overall resistance of the continental lithosphere to extension, we calculated the required boundary force (Figure 4) to keep the constant

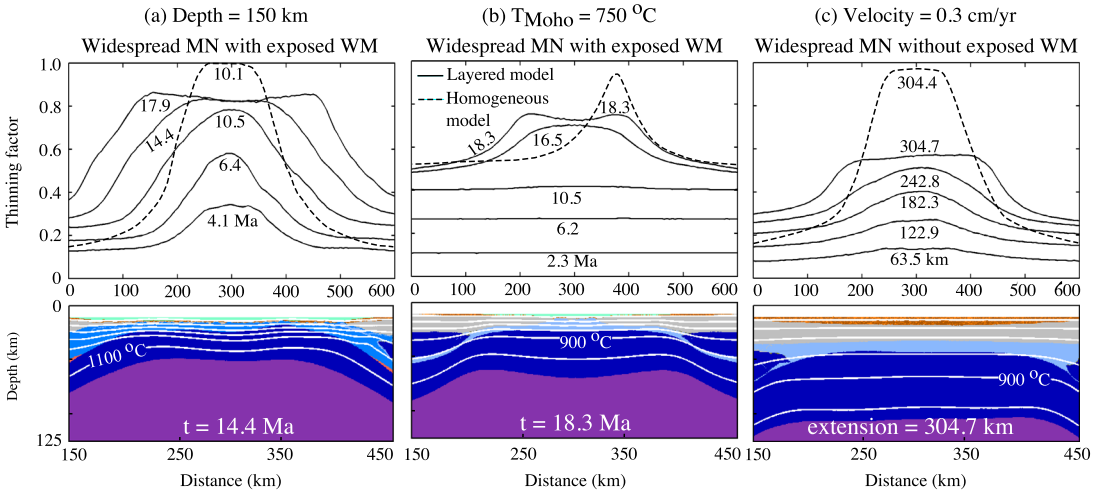

Figure 3. Influence of the (a) weak-layer depth (depth to the surface of the weak layer), (b) Moho temperature, and (c) extension rate on lithospheric extension. Only one parameter is changed in each model compared to the reference models in Figure 2. Dynamic evolution of the models is shown with thinning factor, which is the normalized lithospheric thinning: $(l_0 - l)/l_0$, where l_0 is the original lithospheric thickness, l is the lithospheric thickness at a certain time. When thinning factor reaches 1, lithospheric breakup occurs. Extension amount in Figure 3c is computed by multiplying full extension rate with extension time. One composition snapshot is shown for each layered model (corresponding to the line with the same time in the thinning factor graph). Isotherms are in white lines with an interval of 200°C in the composition snapshots. Note the deformation pattern for each model. MN: mantle necking, WM: weak-layer material.

velocities on the side boundaries (by integrating boundary normal stress across the entire boundary on each side, and taking the mean value between the left and right boundary forces). The boundary force in the layered model is lower than that in the homogeneous model in the early extension stage, implying that the layered model is easier to trigger deformation under the same stress induced by slab pull and/or mantle convection. Rapid force decrease in the early extension stage is caused by the formation of large shear zones cutting through the upper lithosphere, and this force decrease occurs earlier in the layered model because the weak layer enhances the brittle deformation in the upper lithosphere. Due to the formation of mantle necking, boundary force in the layered model can exceed that in the homogeneous model in the late extension stage. Deeper weak layer has less influence on the brittle deformation of the upper lithosphere (Figure 4a). High initial Moho temperatures can significantly reduce the boundary force at the beginning of extension (Figure 4b). The effect of extension rate on the boundary force is not notable (Figure 4c).

4. Discussions and Conclusions

[10] In order to drive the weak-layer flow by pressure gradient, sufficiently low viscosity of the weak layer is required. In our models, the effective viscosity of the weak layer is several orders of magnitude lower than that of the mantle lithosphere. In addition to the relatively weak wet olivine flow law, strong viscosity reduction is caused by strain-rate localization in the weak layer in combination with power law dislocation creep. *Hopper and Buck* [1998] showed that weak flow laws and high temperatures are critical conditions for lower crust flow under extension. Weak-layer flow is typically a consequence of extension, however, if the layered model is subjected to compression, deformation dynamics will dramatically change and delamination of the lithospheric mantle underneath the weak layer will possibly occur [*Gorczyk et al.*, 2012].

[11] The major driving force of plate motion is slab pull, which is one order of magnitude higher than any other forces [*Forsyth and Uyeda*, 1975; *Turcotte and Schubert*, 2002]. The slab pull force computed by *Turcotte and Schubert*

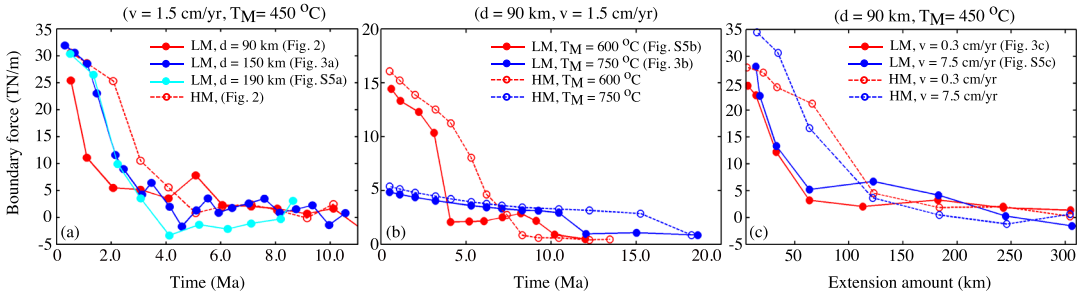

Figure 4. Boundary force evolution for layered models (LM) and homogeneous models (HM) influenced by (a) weak-layer depth, (b) Moho temperature, and (c) extension rate. Symbols used in this figure are the following: v is boundary extension rate (half rate), T_M is Moho temperature, d is weak-layer depth.

[2002] is 33 TN/m (49 TN/m if considering the olivine-spinel phase transition), which is comparable to the peak boundary force in our models (Figure 4). The average stress of cratons subjected to the ongoing mantle convection is several hundreds of megapascal [*O'Neill et al.*, 2008]. A force reduction of 10 TN/m (Figure 4a) corresponds to an average stress reduction of 50 MPa for a cratonic lithospheric thickness of 200 km, which is one order of magnitude smaller than the average cratonic stress. Therefore, although the weak layer can accelerate deformation process, it may not play a dominant role in triggering craton destruction. The most critical condition to initiate extension of a craton is availability of the extension force which is maximal in the beginning (Figure 4). According to our experiments, this peak extension force does not depend significantly on the presence/absence of the weak mantle layer (Figure 4a) but rather on the Moho temperature (Figure 4b). Therefore, onset of extension of layered cratons in nature can be triggered by the Moho temperature increase (especially for young cratons/late Proterozoic lithosphere) [*Artemieva and Mooney*, 2001], for example, due to the plume-induced magmatism, which is often proposed to trigger continental breakup processes [*Kendall et al.*, 2005].

[12] We test how the lithospheric extension patterns of cratons change with a layered mantle structure. The midlithospheric layer enhances the deformation of the overlying mantle and crust, but slows down the upwelling/necking of the underlying mantle. Three dominant patterns of extension are identified: (1) localized mantle necking with exposed weak layer favored by cold Moho temperatures and fast extension rates, (2) widespread mantle necking with exposed weak layer favored by deep weak layers and high Moho temperatures, and (3) widespread mantle necking without exposed weak layer generated only by slow extension rates. The layered model requires a lower boundary force compared to the homogeneous model to sustain a constant boundary extension rate.

[13] **Acknowledgments.** The manuscript has been improved by comments from Norm Sleep and an anonymous reviewer. This work is funded by NSFC project (40872144). J.L. acknowledges funding from China Scholarship Council.

[14] The Editor thanks Norman Sleep and an anonymous reviewer for their assistance in evaluating this paper.

References

Abt, D. L., K. M. Fischer, S. W. French, H. A. Ford, H. Yuan, and B. Romanowicz (2010), North American lithospheric discontinuity structure imaged by *Ps* and *Sp* receiver functions, *J. Geophys. Res.*, *115*, B09301, doi:10.1029/2009JB006914.

Artemieva, I. M., and W. D. Mooney (2001), Thermal thickness and evolution of Precambrian lithosphere: A global study, *J. Geophys. Res.*, *106*(B8), 16,387–16,414.

Carlson, R. W., D. G. Pearson, and D. E. James (2005), Physical, chemical, and chronological characteristics of continental mantle, *Rev. Geophys.*, *43*, RG1001, doi:10.1029/2004RG000156.

Crameri, F., H. Schmeling, G. J. Golabek, T. Duretz, R. Orendt, S. J. H. Buiter, D. A. May, B. J. P. Kaus, T. V. Gerya, and P. J. Tackley (2012), A comparison of numerical surface topography calculations in geodynamic modelling: An evaluation of the 'sticky air' method, *Geophys. J. Int.*, *189*, 38–54, doi:10.1111/j.1365-246X.2012.05388.x.

Eaton, D. W., F. Darbyshire, R. L. Evans, H. Grutter, A. G. Jones, and X. Yuan (2009), The elusive lithosphere–asthenosphere boundary (LAB) beneath cratons, *Lithos*, *109*, 1–22, doi:10.1016/j.lithos.2008.05.009.

Fischer, K. M., H. A. Ford, D. L. Abt, and C. A. Rychert (2010), The lithosphere-asthenosphere boundary, *Annu. Rev. Earth Planet. Sci.*, *38*, 551–575, doi:10.1146/annurev-earth-040809-152438.

Forsyth, D., and S. Uyeda (1975), On the relative importance of the driving forces of plate motion, *Geophys. J. R. Astron. Soc.*, *43*, 163–200.

Gerya, T. V. (2012), Precambrian geodynamics: Concepts and models, *Gondwana Res.*, doi:10.1016/j.gr.2012.11.008, in press.

Gerya, T. V., and D. A. Yuen (2007), Robust characteristics method for modelling multiphase visco-elasto-plastic thermo-mechanical problems, *Phys. Earth Planet. Inter.*, *163*, 83–105, doi:10.1016/j.pepi.2007.04.015.

Gorczyk, W., B. Hobbs, and T. Gerya (2012), Initiation of Rayleigh-Taylor instabilities in intra-cratonic settings, *Tectonophysics*, *514-517*, 146–155, doi:10.1016/j.tecto.2011.10.016.

Griffin, W. L., S. Y. O'Reilly, L. M. Natapov, and C. G. Ryan (2003), The evolution of lithospheric mantle beneath the Kalahari Craton and its margins, *Lithos*, *71*, 215–241, doi:10.1016/j.lithos.2003.07.006.

Griffin, W. L., S. Y. O'Reilly, B. J. Doyle, N. J. Pearson, H. Coopersmith, K. Kivi, V. Malkovets, and N. Pokhilenko (2004), Lithosphere mapping beneath the North American plate, *Lithos*, *77*, 873–922, doi:10.1016/j.lithos.2004.03.034.

Gueydan, F., C. Morency, and J.-P. Brun (2008), Continental rifting as a function of lithosphere mantle strength, *Tectonophysics*, *460*, 83–93, doi:10.1016/j.tecto.2008.08.012.

Hacker, B. R., S. M. Peacock, G. A. Abers, and S. D. Holloway (2003), Subduction factory 2. Are intermediate-depth earthquakes in subducting slabs linked to metamorphic dehydration reactions?, *J. Geophys. Res.*, *108*(B1), 2030, doi:10.1029/2001JB001129.

Hopper, J. R., and W. R. Buck (1998), Styles of extensional decoupling, *Geology*, *26*, 699–702, doi:10.1130/0091-7613(1998)026<0699:SOED>2.3.CO;2.

Huismans, R., and C. Beaumont (2011), Depth-dependent extension, two-stage breakup and cratonic underplating at rifted margins, *Nature*, *473*, 74–79, doi:10.1038/nature09988.

Karato, S., and H. Jung (1998), Water, partial melting and the origin of the seismic low velocity and high attenuation zone in the upper mantle, *Earth Planet. Sci. Lett.*, *157*, 193–207.

Kendall, J.-M., G. W. Stuart, C. J. Ebinger, I. D. Bastow, and D. Keir (2005), Magma-assisted rifting in Ethiopia, *Nature*, *433*, 146–148, doi:10.1038/nature03161.

Lee, C.-T. A., P. Luffi, and E. J. Chin (2011), Building and destroying continental mantle, *Annu. Rev. Earth Planet. Sci.*, *39*, 59–90, doi:10.1146/annurev-earth-040610-133505.

Lenardic, A., and L.-N. Moresi (1999), Some thoughts on the stability of cratonic lithosphere: Effects of buoyancy and viscosity, *J. Geophys. Res.*, *104*(B6), 12,747–12,758.

Lenardic, A., L. Moresi, and H. Mühlhaus (2000), The role of mobile belts for the longevity of deep cratonic lithosphere: The Crumple Zone Model, *Geophys. Res. Lett.*, *27*(8), 1235–1238.

Lenardic, A., L.-N. Moresi, and H. Mühlhaus (2003), Longevity and stability of cratonic lithosphere: Insights from numerical simulations of coupled mantle convection and continental tectonics, *J. Geophys. Res.*, *108*(B6), 2303, doi:10.1029/2002JB001859.

Maumus, J., N. Bagdassarov, and H. Schmeling (2005), Electrical conductivity and partial melting of mafic rocks under pressure, *Geochim. Cosmochim. Acta*, *69*(19), 4703–4718, doi:10.1016/j.gca.2005.05.010.

O'Neill, C. J., A. Lenardic, W. L. Griffin, and S. Y. O'Reilly (2008), Dynamics of cratons in an evolving mantle, *Lithos*, *102*, 12–24, doi:10.1016/j.lithos.2007.04.006.

O'Neill, C. J., A. Kobussen, and A. Lenardic (2010), The mechanics of continental lithosphere-asthenosphere coupling, *Lithos*, *120*, 55–62, doi:10.1016/j.lithos.2010.07.008.

Peltonen, P., and G. Brügmann (2006), Origin of layered continental mantle (Karelian craton, Finland): Geochemical and Re–Os isotope constraints, *Lithos*, *89*, 405–423, doi:10.1016/j.lithos.2005.12.013.

Peslier, A. H., A. B. Woodland, D. R. Bell, and M. Lazarov (2010), Olivine water contents in the continental lithosphere and the longevity of cratons, *Nature*, *467*, 78–81, doi:10.1038/nature09317.

Romanowicz, B. (2009), The thickness of tectonic plates, *Science*, *324*, 474–476, doi:10.1126/science.1172879.

Rychert, C. A., and P. M. Shearer (2009), A global view of the lithosphere-asthenosphere boundary, *Science*, *324*(5926), 495–497, doi:10.1126/science.1169754.

Sleep, N. H. (2005), Evolution of the continental lithosphere, *Annu. Rev. Earth Planet. Sci.*, *33*, 369–93, doi:10.1146/annurev.earth.33.092203.122643.

Sleep, N. H. (2009), Stagnant lid convection and carbonate metasomatism of the deep continental lithosphere, *Geochem. Geophys. Geosyst.*, *10*, Q11010, doi:10.1029/2009GC002702.

Thybo, H. (2006), The heterogeneous upper mantle low velocity zone, *Tectonophysics*, *416*, 53–79, doi:10.1016/j.tecto.2005.11.021.

Thybo, H., and E. Perchuc (1997), The seismic 8° discontinuity and partial melting in continental mantle, *Science*, *275*(5306), 1626–1629, doi:10.1126/science.275.5306.1626.

Turcotte, D. L., and G. Schubert (2002), *Geodynamics*, Cambridge Univ. Press, Cambridge, U. K.

Wang, Q. (2010), A review of water contents and ductile deformation mechanisms of olivine: Implications for the lithosphere–asthenosphere boundary of continents, *Lithos*, *120*, 30–41, doi:10.1016/j.lithos.2010.05.010.

Wang, Q., N. Bagdassarov, Q.-K. Xia, and B. Zhu (2013), Water contents and electrical conductivity of peridotite xenoliths from the North China Craton: Implications for water distribution in the upper mantle, *Lithos*, doi:10.1016/j.lithos.2013.08.005, in press.

Yoshida, M. (2012), Dynamic role of the rheological contrast between cratonic and oceanic lithospheres in the longevity of cratonic lithosphere: A three-dimensional numerical study, *Tectonophysics*, *532-535*, 156–166, doi:10.1016/j.tecto.2012.01.029.

Yuan, H., and B. Romanowicz (2010), Lithospheric layering in the North American craton, *Nature*, *466*, 1063–1068, doi:10.1038/nature09332.